Variations in Supercell Morphology. Part I: Observations of the Role of Upper-Level Storm-Relative Flow

ERIK N. RASMUSSEN

Cooperative Institute for Mesoscale Meteorological Studies, National Severe Storms Laboratory, NOAA, and University of Oklahoma, Norman, Oklahoma

JERRY M. STRAKA

School of Meteorology, University of Oklahoma, Norman, Oklahoma

(Manuscript received 3 September 1996, in final form 21 November 1997)

ABSTRACT

It is hypothesized that the precipitation intensity beneath a supercell updraft is strongly influenced by the amount of hydrometeors that are reingested into the updraft after being transported away in the divergent upper-level flow of the anvil. This paper presents the results of a climatological analysis of soundings associated with three types of isolated supercells having distinctive precipitation distributions, the so-called classic, low-precipitation (LP), and high-precipitation (HP) storms. It is shown that storm-relative flow at 9–10 km above the ground is strongest in the environments of LP storms, and relatively weak in the environments of HP storms, with classic storms occurring in environments with intermediate magnitudes of upper storm-relative flow. It is plausible that comparatively strong flow in the anvil-bearing levels of LP storms transports hydrometeors far enough from the updraft that they are relatively unlikely to be reingested into the updraft, leading to greatly diminished precipitation formation in the updraft itself. Conversely, the weak upper flow near HP storms apparently allows a relatively large number of hydrometeors to return to the updraft, leading to the generation of relatively large amounts of precipitation in the updraft. It also is apparent that thermodynamic factors such as convective available potential energy, low-level mixing ratio, and mean relative humidity are of lesser importance in determining storm type from a climatological perspective, although important variations in humidity may not be well sampled in this study. This climatological analysis does not directly evaluate the stated hypothesis; however, the findings do indicate that further modeling and microphysical observations are warranted.

1. Introduction

a. Supercell definition

Most recent definitions of supercells incorporate the requirement for a deep, persistent mesocyclone, and a large degree of correlation between the mesocyclone and an updraft (e.g., Klemp 1987; Doswell and Burgess 1993; Brooks et al. 1994b), and hence some commonality in the dynamics of these storms is likely (e.g., Rotunno and Klemp 1982, 1985; Weisman and Klemp 1982, 1984). From an operational viewpoint, it is not possible to directly determine the degree of correlation between vertical velocity and vorticity because real-time information on vertical velocity in storms is not available using present technology, so those storms containing deep, persistent mesocyclones[1] must be assumed to be supercells (Moller et al. 1994).

Lost in this definition is the notion that precipitation distribution is not just a manifestation of the unique airflow in supercells, but that it may play a key role in generation of the mesocyclones and tornadoes. Indeed, current definitions of what constitutes a supercell do not incorporate the nature of the storm precipitation at all. Recent numerical simulation work has just begun to illuminate the importance of precipitation physics, especially evaporation and the strength and location of the cold pool, in supercell dynamics. For example, Brooks et al. (1994b) have found evidence that the mesocyclone and storm-relative flow can alter the location and intensity of the evaporatively driven cold pool and the nature of low-level mesocyclone genesis. Although the

Corresponding author address: Erik Rasmussen, NSSL/NOAA 3450 Mitchell Lane, Bldg. 3, Room 2034, Boulder, CO 80301.
E-mail: rasmussen@nssl.noaa.gov

[1] It seems the presence of a deep, persistent mesoanticyclone should also be included in the operational criteria for supercell identification because simulated left-moving members of storm split pairs in straight shear have been shown to be mirror-image supercells (Wilhelmson and Klemp 1978).

findings presented herein do not agree entirely with those of Brooks et al. (1994b) as to the cause of variations in the precipitation distribution between the so-called classic (CL) and high-precipitation (HP) supercells (defined later), the cold pool strength and location does seem to be of fundamental importance. Further evidence for the dependence of supercell dynamics and tornadogenesis on cold pool characteristics can be found in Davies-Jones and Brooks (1993). It is plausible that storm propagation, low-level mesocyclone formation and demise, and even midlevel mesocyclone rotation are all dependent to some degree on the location and strength of low-level horizontal gradients of buoyancy, and these in turn are strongly dependent on the precipitation distribution in the storm.

The frequently observed patterns of the spatial distribution of precipitation, and the inferred motion fields, were fundamental in some of the earliest studies of supercells (Browning and Donaldson 1963; Browning 1964). Eventually, some of the reflectivity patterns documented in these studies became the basis for operational detection of supercell storms (Lemon 1982). The directly observed rotating wind field increased in importance as a result of the use of Doppler radar in research, as well as numerical simulations. However, the precipitation processes and structure have been largely ignored as a research topic until quite recently. In light of the known propensity for CL supercells to produce tornadoes, the tendency of HP supercells to produce severe winds and large hail (Moller et al. 1994), and the relative rarity of tornadoes with low-precipitation (LP) storms, it is appropriate to re-examine precipitation physics and the associated effects on storm dynamics. It cannot be assumed that all storms having a deep, persistent mesocyclone have the same propagation characteristics, potential for severity, etc.

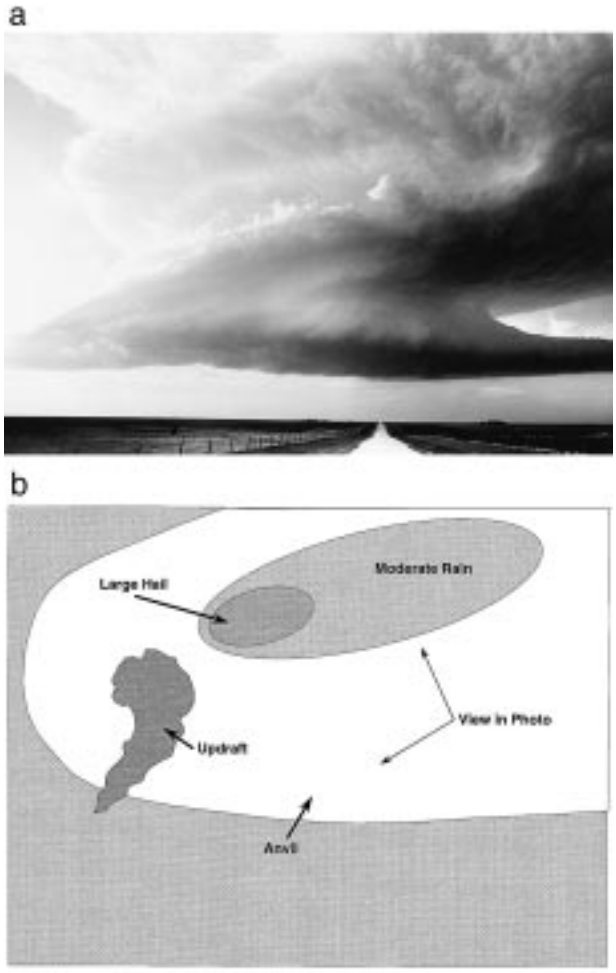

FIG. 1. (a) Photograph of an LP supercell and (b) schematic diagram of LP supercells that occurred in the Texas panhandle on 28 May 1994 (photo courtesy of W. Faidley, Weatherstock). View to the west.

b. The supercell spectrum

Since the first supercell thunderstorm descriptions (e.g., Browning 1964), at least three types of supercells including LP (e.g., Burgess and Davies-Jones 1979; Bluestein and Parks 1983), CL (e.g., Browning 1964; Lemon and Doswell 1979), and HP (e.g., Doswell et al. 1990; Moller et al. 1994) have been described. These are identified by the amount of precipitation they produce, and where the precipitation is deposited relative to their respective updrafts. Observations indicate that these are really archetypal storms; actual storms fill a spectrum of types (Doswell et al. 1990), and there presently is no evidence of modes in the spectrum near the archetypes. Furthermore, an LP supercell may evolve into the classic form, and finally into an HP storm (Bluestein and Woodall 1990).

The first formal report of what appears to be an LP supercell storm is from the early 1960s. Since then, more than a dozen of these storms have been described in varying degrees of detail in the reviewed literature. A statistical examination of supercell environments by Bluestein and Parks (1983) found slightly weaker low- and midlevel environmental shears and little difference in convective available potential energy (CAPE). The typical LP supercell is characterized by a relative absence of rain in and near a deep rotating updraft, and by the occurrence of light to moderate rain and/or large hail falling from the anvil (Donaldson et al. 1965; Marwitz 1972; Davies-Jones et al. 1976; Burgess and Davies-Jones 1979; Bluestein and Parks 1983; Bluestein 1984; Bluestein and Woodall 1990). These storms appear as laminar bell-shaped columnar cumulus towers with long streaming anvils. Bluestein and Parks (1983) have likened the visual appearance of an LP supercell to the skeleton of a classic supercell (Fig. 1). Midlevel funnels from the convective towers of LP storms often are observed. Owing to a lack of precipitation, strong hydrometeor-induced downdrafts are not observed with these storms. In addition, tornadoes are rarely produced by LP storms (Bluestein and Parks 1983;

Doswell and Burgess 1993), though they have been documented (Davies-Jones et al. 1976; Burgess and Davies-Jones 1979). At least one of these accounts is associated with the merger of an LP and HP supercell (Davies-Jones et al. 1976). As LP storms are usually observed near a dryline in the spring over the Southern Plains, they are highly visible owing to sparse precipitation and a lack of extensive midlevel cloudiness (Doswell and Burgess 1993). Updraft rotation in LP storms may be difficult to detect with Doppler owing to a lack of large enough precipitation particles in the updraft and mesocyclone (Doswell and Burgess 1993); low-level hook echoes should not exist.

One of the first attempts to produce a three-dimensional numerical simulation of an LP supercell is that reported by Weisman and Bluestein (1985). They found that LP-like storms could be simulated if the precipitation microphysics are turned off in their model. In essence they demonstrated that simulated supercells could be sustained in weak low-level shear environments if mechanisms associated with precipitation did not interfere with the dynamics of the storm. From their experiments, Weisman and Bluestein hypothesized that certain microphysical ingredients, such as those associated with the nucleation of ice crystals and cloud droplets, might be different near the dryline (e.g., larger concentrations of condensation nuclei and ice nuclei) where LP supercells usually are observed. Axisymmetric simulations by Proctor (1983) of intense convective cells that produce little precipitation at the surface suggest that strong updrafts prevent precipitation from falling through updrafts in LP storms. More recently, Brooks and Wilhelmson (1992) simulated what they called an LP supercell without artificially suppressing precipitation processes as done by Weisman and Bluestein (1985). They attributed their apparent success to using a smaller initial thermal perturbation to trigger convection in an environment that would typically require a larger initial thermal perturbation to induce a classic supercell. This idea supports an earlier speculation by Bluestein and Parks (1983). However, Brooks and Wilhelmson's LP supercell simulation is not entirely consistent with observations of the LP supercell that formed in nature in the environment they used to initialize their model. Most important, their simulated storm did not contain as significant an updraft (maximum updraft of <10 m s^{-1} in the LP supercell stage) as was observed (maximum of 35 m s^{-1}; Bluestein and Woodall 1990). The likely reason that their simulated storm appeared to be an LP supercell (produced less amounts of precipitation at the surface than their simulation initiated with a larger bubble) is that it had no strong updrafts, and thus produced small amounts of precipitation.

Classic supercell storms are the most prolific producers of severe weather phenomena such as large hail and major tornadoes. The conceptual classic supercell models (Fig. 2) described by Browning (1964) and Lemon and Doswell (1979) are still considered valid. These types of storms are thought to form in environments with substantial low- and midlevel shear; stronger shear apparently is required when CAPE is small than when it is large (Johns et al. 1993). Using numerical simulations and observations, Brooks et al. (1994b) suggest that classic supercell storms are associated with substantial midlevel (3–7 km) environmental wind shear. The visual appearance of these storms usually is such that the updraft is highly visible and basically precipitation free, except for some precipitation wrapping around the left side and rear (looking along the direction of storm motion) of the updraft. A precipitation shield downshear from the updraft also is readily visible. As some precipitation usually is present in the updrafts of these storms their mesocyclones are detectable in the wind fields observed with Doppler radar, and typically produce a ''hook echo'' in the reflectivity field (Forbes 1981). Doswell and Burgess (1993) state that reflectivities in the hook echo of a CL supercell are less than in the precipitation core, where values are largest just

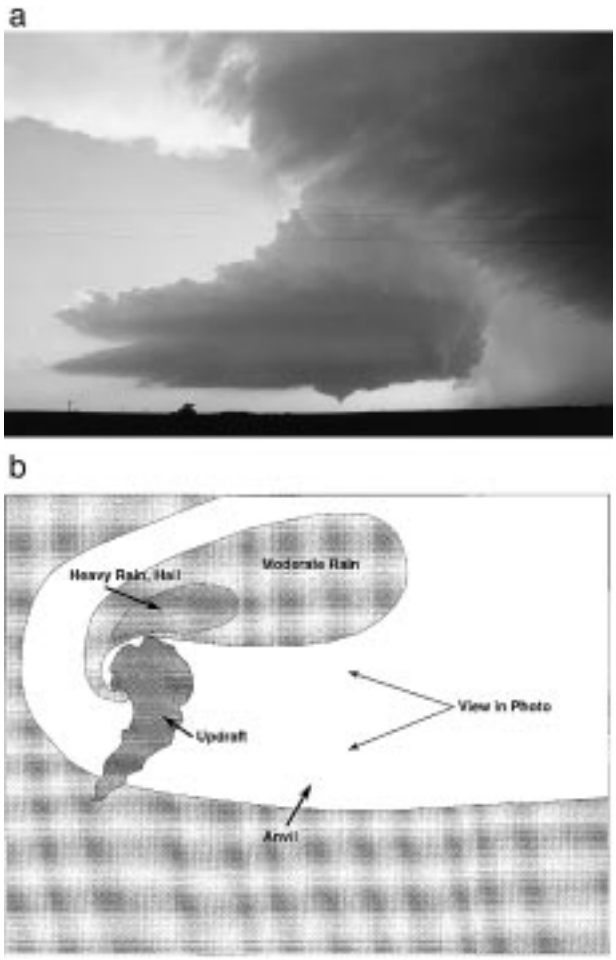

FIG. 2. (a) Photograph of a classic supercell and (b) schematic diagram of CL supercells that occurred near Alma, Nebraska, on 30 May 1991 (photographed by E. Rasmussen). View toward the west.

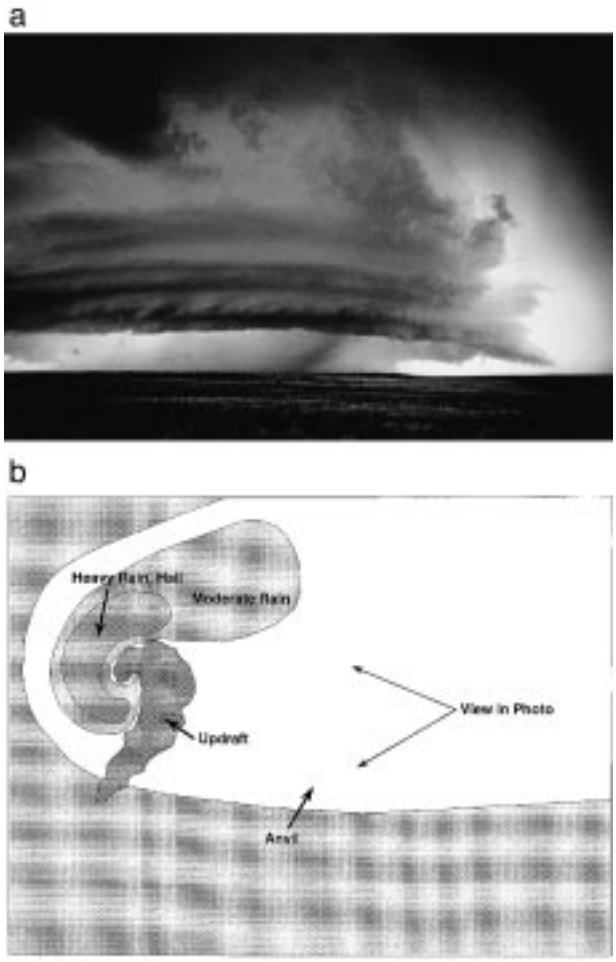

FIG. 3. (a) Photograph of an HP supercell and (b) schematic diagram of HP supercells that occurred in southwest Oklahoma on 19 April 1992 (photographed by P. Spencer). View toward the west.

to the left of the updraft path owing to heavy rain and often very large hail.

Idealized simulations of CL supercell storms are numerous in the literature, including, most notably, those by Wilhelmson and Klemp (1978), Klemp et al. (1981), Weisman and Klemp (1982, 1984, 1986), Klemp and Rotunno (1983), and Brooks et al. (1994b). Enough physics is contained in these simulations to be able to capture strong low- and midlevel rotation, rear- and forward-flank downdrafts, and typical radar appearance including the hook echo, weak echo region, and v notch.

The HP supercell is the latest supercell category to be described in the literature (e.g., Moller et al. 1990; Moller et al. 1994; Doswell and Burgess 1993; Brooks et al. 1994b; Brooks et al. 1994a). Moller et al. (1990) state that the HP type is the most common supercell form, and can develop in all regions of the United States. High-precipitation supercells are known to produce noteworthy flash flood events, and occasionally produce large hail, damaging winds, and tornadoes. Visually (Fig. 3), HP supercells can be very difficult to observe as they usually form in humid, cloud-filled environments (Doswell and Burgess 1993). When they are isolated in relatively cloud-free environments they have the visual appearance of a rotating semiannular updraft (open to the rear) with rain in the middle, a possible wall cloud on the forward left side of the updraft (looking along the storm motion vector), and often intense precipitation under the forward anvil region as well. A distinguishing radar characteristic of this storm type is that significant updraft precipitation makes their mesocyclones prominent. However, the heavy precipitation in the updraft can make it very difficult to observe the mesocyclone and possible embedded tornadoes visually. Typically, reflectivities in the hook echo, if one is present, may be as large or larger than in the precipitation core of the storm. In addition, hook echoes may be very large and full of precipitation, so the storm may appear more like a kidney bean in shape. The structures of HP supercells can be quite varied often making them hard to identify without Doppler data (Doswell et al. 1990).

Brooks et al. (1994b) suggest that HP supercells form in the typical supercell environment, except that the midlevel storm-relative wind speed (3–7 km) is relatively small. They claim that because of significant low- and midlevel rotation and a weakness in midlevel shear, the mesocyclone circulation can carry precipitation, which typically falls downshear in CL storms, around to the rear and through the updraft. This explanation is plausible; however, the present study associates weak midlevel storm-relative flow with LP storms and finds that the midlevel flow in isolated HP and CL supercells is stronger (see section 3).

The studies discussed above generally adhere to a classification scheme that is in some ways not adequate to describe the important aspects of the variations in structure and dynamics among supercells. In general, earlier studies seem to imply that it is the precipitation intensity beneath the updraft that determines the supercell type, but there is some ambiguity regarding the importance of the precipitation rate beneath the forward flank anvil. For instance, it is unclear whether a storm having little precipitation below the updraft, but heavy precipitation in the forward flank, would be classified as LP or another type. From an observational perspective, very little attention has been paid to the precipitation rate below the forward flank, and the important dynamical role it has.

In this paper, the current nomenclature is retained because it is the distribution of precipitation below the updraft that is of interest. Further research is needed to quantify, based on radar observations or in situ measurements, the frequency spectrum of updraft region and forward-flank region precipitation rates. Indeed, a weakness of most previous studies (as well as this one) pertaining to the supercell spectrum is the use of subjective impressions of precipitation intensity based on visual observations. The authors have seen several photographs purporting to show tornadic LP storms, which

in fact show storms with obvious thin veils of precipitation beneath the updraft and near the tornadoes. One must wonder whether or not these are true LP storms, and whether the tornadoes would be in existence if they were!

c. Hypothesis

In Part II of this paper, a simple hypothesis is evaluated; a primary cause of the variations of storm morphology across the supercell spectrum, observed as differences in the distribution and intensity of precipitation near the updraft, is the degree to which storm updrafts reingest hydrometeors that descend from the upper regions of the storm (i.e., diverging anvil) or from other storms. A corollary to this hypothesis is that the HP supercell should be the most common type of supercell *if* it is true that storms are rarely completely isolated and instead often have nearby storms providing hydrometeors to be reingested. A second corollary is that LP storms are most likely when there are no storms upstream to introduce hydrometeors into the updrafts of the supercells; this condition is most likely near the High Plains dryline or at the upstream end of lines of supercells. These corollaries will be discussed in more detail in section 4.

Numerous studies that investigate the formation of precipitation (especially hail) in severe thunderstorms have been published (e.g., Browning and Foote 1976; Browning 1977; Paluch 1978; Ziegler et al. 1983; Foote 1984; Knight and Knupp 1986; Miller et al. 1988; Miller et al. 1990). However, many of these deal with nonsupercell convection or describe supercells that are not easily classified using the emerging nomenclature discussed above. A few findings are pertinent to the present study. For instance, several case studies (Foote 1984; Knight and Knupp 1986; Miller et al. 1988) of supercell-like storms clearly indicate that a hailstone usually grows after an embryo reenters the updraft and makes a single pass through it. Hail embryos can be shown to originate in several parts of the storm, including the forward flank, periphery of the updraft, and the upstream convective turrets and stagnation region. Knight and Knupp (1986) were able to show preferred origin zones for several fallout regions; for example, hail that falls in the hook echo has possible origins in the upstream stagnation zone in the storm they investigated. Despite the findings of these studies, the existing body of observational evidence for precipitation processes in supercells is much too limited to make generalizations about the causes of the supercell spectrum. The hypothesis that is the subject of the present investigation does not specify where precipitation embryos first grow to embryonic size (i.e., millimeter) nor where they reenter the updraft. Instead, it is assumed that wherever the embryos form, it is much more likely that they will reenter the updraft if upper-level storm-relative flow is weak, and less likely if it is strong. This is important because it is quite likely that embryos that descend near the updraft will reenter it owing to the generally convergent flow in the vicinity of the lower one-half of the updraft (Foote 1984).

To determine if there is evidence in the storm environments to support the hypothesis, the environments of 43 supercell cases were examined. The findings of this analysis are reported in this paper, which is the first part of a two-part series. In section two, the methods used in this climatological analysis are described, with the results discussed in sections three and four. In Part II, numerical simulations are used to evaluate the hypothesis presented above, a conceptual model of the fundamental physical causes of the varying morphology across the supercell spectrum is presented, and the implications for storm forecasting, recognition, and tornado production are examined further.

2. Methods of analysis

a. Case selection

Forty-three cases were selected that seem to typify the three archetypes in the supercell spectrum described above. To be selected, an LP storm must have had little or no precipitation visible near the storm updraft (Bluestein and Parks 1983), and the updraft must have shown obvious rotation visually (i.e., a supercell). Storms with intermediate intensities of precipitation beneath the updraft are classified as ''classic'' and must have had the dominant precipitation area under the downshear anvil, with some precipitation near the updraft on the left and rear sides, possibly including a curtain of precipitation surrounding a tornado (depicted by radar as a hook echo), but not obscuring it from view. Storms classified as HP must have had extensive precipitation near and to the rear of the updraft (with respect to storm motion), with tornadoes and wall clouds generally obscured by precipitation (although the edge of the updraft was usually visible, and showed overall updraft rotation). All of the storms selected for this analysis were observed by the authors, were described to the authors by very experienced observers of supercells, or have been the subject of published studies (the cases chosen are listed in Table 1 with the source of the information used to classify the storms). To avoid some of the subjectivity associated with visual observations of precipitation intensity, *storms that were between these archetypes, and thus hard to classify, were excluded from the analysis.*

If the hypothesis is correct, most supercells that develop as isolated updrafts in regions without thick cirrus canopies should be LP storms for at least a brief time (~20–40 min) at the beginning of their life cycles, and then may progress toward the HP end of the spectrum as increasing numbers of hydrometeors are reingested into the updraft. For this analysis, storms are classified according to the structure that dominates the life cycle. If a storm did not evolve to a structure close to one of

TABLE 1. List of storms included in the analysis. Here CL denotes classic, HP denotes high precipitation, and LP denotes low precipitation supercells. The ''source'' column lists the source of the information used to classify each storm.

Type	Location	Date	Source
CL	Tecumseh, OK	17 May 1981	Authors
	Binger, OK	22 May 1981	Authors
	Hesston, KS	13 March 1990	Photographs
	Red Rock, OK	26 April 1991	Authors
	Pampa, TX	19 May 1982	Authors
	Grand Island, NE	3 June 1980	Photographs
	Broken Bow, NE	1 June 1990	Authors
	Alma, NE	30 May 1991	Authors
	Hooker, TX	5 May 1993	Photographs
	Wichita Falls, TX	10 April 1979	Authors
	Great Bend, KS	24 May 1990	Photographs
	Western KS	25 April 1990	Photographs
	Houston, TX	21 November 1992	Photographs
	Enid, OK	12 April 1991	G. Stumpf, personal communication
	Geary, OK	15 May 1990	G. Stumpf, personal communication
	Hays, KS	10 May 1985	Authors
	Tulia, TX	28 May 1980	Authors
HP	Goodland, KS	28 June 1989	Authors
	Kaw Res., OK	6 May 1994	Authors
	Altus, OK	7 June 1993	Authors
	Southern NE	16 June 1990	Authors
	Purcell, OK	2 September 1992	Authors
	Katie, OK	23 May 1981	Authors
	North TX	28 April 1982	Photographs
	Memphis, TX	11 May 1982	Authors
	Beloit, KS	15 June 1992	Authors
	Orla, TX	22 May 1992	G. Stumpf, personal communication
	Tulsa, OK	24 April 1993	Authors
	Lahoma, OK	17 August 1994	Photographs
	Wellington, TX	29 May 1980	Authors
LP	Dodge City, KS	30 May 1978	Authors
	Wilbarger, TX	13 May 1989	G. Stumpf, personal communication
	Texas panhandle	18 May 1990	G. Stumpf, personal communication
	Illiff, CO	1 July 1989	D. Blanchard
	Lamar, CO	1 July 1989	Authors
	Oklahoma	4 June 1973	Davies-Jones et al. (1976)
	Western TX	26 April 1976	Bluestein and Parks (1983)
	Western TX	27 April 1976	Bluestein and Parks (1983)
	Norman, OK	20 June 1979	Bluestein and Parks (1983)
	MacDonald, KS	1 July 1993	D. Blanchard, personal communication
	Ft. Morgan, CO	15 June 1970	Marwitz (1972)
	Lubbock, TX	25 May 1994	D. Baker, personal communication

the archetypes in a relatively short amount of time, or exhibited the archetypal structure for less than an hour, it was excluded.

One criterion of prime importance in case selection is that the storm must have been isolated from other storms, and their anvils. This requirement was especially cumbersome; most HP storms were eliminated from consideration when it was found that there were nearby and upstream supercells that may have been depositing hydrometeors into the HP storm's updraft. In this observational study, the goal is to isolate the role of the environment, not investigate storm interactions. Although the HP may be the most common type of supercell, it seems that *isolated* HP storms are one of the least common varieties of supercells. It is hypothesized that interaction between storm updrafts and anvils of other storms will invariably move a storm toward the HP end of the spectrum (this is investigated numerically in Part II).

Two techniques were used to assign storm motions for the cases examined. If storm intercept field notes indicate the locations and times of the updraft, these were used to determine the storm motion. Otherwise, coded National Weather Service radar observations obtained through the National Climatic Data Center were examined to determine the motion of the storm during its mature stage by plotting observed storm centroids versus time. The motions determined through either of these techniques should be accurate to within 2–3 m s^{-1} (the errors likely are random, not systematic).

b. Sounding selection

The selection of a sounding that is ''representative'' of the environment of a given storm is a difficult, sub-

jective process (e.g., Maddox 1976; Bluestein and Parks 1983). Brooks et al. (1994a) provide a good discussion of the many issues that must be considered in the sounding selection process. One result of the present study is that supercell type is strongly dependent on storm-relative (hereafter SR) upper-tropospheric flow. It is likely that upper-tropospheric flow varies more slowly in time and space than a quantity such as SR environmental helicity (hereafter SRH; Davies-Jones 1984), which depends strongly on local backing of low-level flow, the enhanced curvature resulting from low-level jets, the presence of mesoscale low-level baroclinity, and other mesoscale phenomenon. Thus, in this study, the emphasis is on selecting, and, if necessary modifying, a sounding to be representative of the storm environment, rather than finding a ''proximity'' sounding.

In general, for each case the closest sounding to the storm that was in the same air mass as the storm, and clearly was not modified by convection, was selected using methods similar to Bluestein and Parks (1983). Some obvious signs of nearby convection include low-level stabilization due to outflow, and middle- and upper-tropospheric warming and moistening associated with anvil clouds. In two cases, soundings just upstream of the supercell were rejected because upper flow had the appearance of being strongly ''blocked'' or deflected by the nearby storm. If necessary, the surface temperature and dewpoint were adjusted to be consistent with conventional hourly surface observations near the storm. In a few cases the boundary layer winds were modified to be consistent with observed surface winds near the storm. Otherwise, winds were not adjusted from the reported values. The guiding philosophy in sounding selection was that if the hypothesis concerning the supercell spectrum was correct, the ''signal'' should be obvious in the soundings without significant refinement of the reported quantities, and without ''picking and choosing'' soundings that best supported the hypothesis. The quantities found to be important in predicting storm type (section 3) are not affected by the modifications to low-level conditions described above. Soundings at 0000 UTC were used; in general these were obtained within 3 h of the mature phases of the storms.

A large number of sounding-derived parameters were analyzed to determine their association with supercell type. This work was done in order to determine suitable alternate hypotheses in case the hypothesis discussed in section 1c was rejected. Table 2 lists most of the parameters that were investigated, and the methods of computation.

3. Results

In this section, the results of the examination of the soundings for the three classes of (isolated) supercells are presented. Some of the sounding-derived parameters computed in this study can be compared to those reported by Bluestein and Parks (1983; hereafter BP). BP's category called supercell is equivalent to our CL class (or perhaps a combination of HP and CL storms), and their ''LP storm'' class is equivalent to our LP category. Results herein should be expected to differ from BP because of differences in sample size, categorization, and methodology.

a. Thermodynamic parameters

As in BP, the heights of the lifting condensation level (LCL; see Table 2 for parameter definition) and level of free convection (LFC) were evaluated. The LCL is not significantly different (as determined using Student's t-test at 95% confidence level) among the three classes of supercells, and ranges from 1200 to 1400 m (Fig. 4). This differs from the BP finding of a significant difference, with LCL heights near 1800 m for LP storms. Again in contrast to BP, the height of the LFC is significantly different between the three classes of storms, with CL storm environments having a much lower LFC ($\sim$1700 m) than those of HP and LP storms ($\gtrsim$2200 m). The fact that the LFC is closer to the LCL in the environment of CL storms implies that the inhibition is smaller and/or the lapse rate is larger above the LCL. Obviously, LFC and LCL heights are sensitive to the low-level distribution of temperature and water vapor, which can vary greatly on the mesoscale; the values computed herein are more representative of large-scale conditions than the conditions at the supercells.

In the present climatology, CAPE is found to be significantly less in LP environments than in those of CL and HP storms (Fig. 4). CAPE averages 2900 J kg^{-1} in the LP environments, a value not too different from that reported by BP (3072 J kg^{-1}). CAPE is largest in the environments of CL and HP storms (about 3700 and 3500 J kg^{-1}, respectively). Various measures of downdraft CAPE are not significantly different (95% level) among the storm types (not shown).

b. Moisture parameters

It has been postulated (Doswell and Burgess 1993) that HP supercells are associated with large amounts of water vapor in the environment. The notion that the ''high precipitation'' character of these storms is the result of large amounts of precipitable water does seem intuitive. The soundings associated with HP occurrence in this study are not significantly more humid than their CL and LP counterparts (Fig. 5) in terms of mean relative humidity. However, the HP soundings show significantly more precipitable water than in CL and LP environments. In BP, CL storms also were found to be in environments with significantly more precipitable water. Since the BP supercell class may include both CL and HP storms, this result is similar to the findings of the present study. That HP storms occur in environments with similar relative humidity but larger precip-

TABLE 2. Table of sounding-derived quantities evaluated in this study.

Quantity	Method of computation
CAPE	Doswell and Rasmussen (1994)
dCAPE from Z = 1, 2, 3, 4, 5, and 6 km. Parcel process (T_p) is saturated pseudoadiabatic descent at the minimum wet bulb potential temperature found above the parcel level. T_e is environment temperature; g is gravity.	$d\text{CAPE} = \int_0^Z g\frac{(T_p - T_e)}{T_e}\,dz$
w_z; adiabatic updraft velocity at 0°C, −40°C.	$w_z = w_0 + (2\text{CAPE})^{0.5}$
τ_z; the parcel residence time below height z, assuming pseudoadiabatic vertical velocity and w_0 = 1 m s^{-1}.	Elapsed time at each height level below z is summed during the CAPE calculation.
T_{CP}; the cold pool temperature deficit at the surface using the parcel process described for dCAPE.	$T_{CP} = (T_p - T_e)_{z=0}$
Mean RH; 0–5 km, 3–9 km.	Depth-weighted mean of RH at reported levels.
PW; precipitable water. q_v is the mixing ratio of vapor and ρ_l is the density of liquid water, and ρ is the density of air.	$\text{PW} = \frac{1}{\rho_l}\int_0^{5\text{ km}} q_v\rho\,dz$
q_{vo}; mixing ratio of the most potentially buoyant parcel.	See Doswell and Rasmussen (1994).
E_p; the evaporation potential. Measures how much water must be evaporated into a column of environmental air to bring it to saturation. Evaluated layers: 0–9 km, 2–9 km, 4–9 km. q_{WB} is the mixing ratio at the wet-bulb temperature.	$E_p = \frac{1}{\rho_l}\int_{Z_0}^{Z_T} \rho(q_{\text{WB}} - q_e)\,dz$
z_E; the evaporation level. This is the height at which a fixed quantity of liquid (M_i) completely evaporates after descending from an initial height (Z_i; 9 km), while bringing all intervening levels to saturation. It is an indicator of net evaporation potential.	$M_i = \frac{1}{\rho_l}\int_{Z_e}^{Z_i} \rho(q_{\text{WB}} - q_e)\,dz$
Z_{LCL}, Z_{LFC}, $Z_{0°\text{C}}$, and $Z_{-40°\text{C}}$; the heights of the lifting condensation level, level of free convection, updraft 0°C and −40°C levels.	Standard.
u, v wind components in boundary layer (0–500 m AGL), at 1, 2, . . . , 9 km, mean in mixed-phase region (0°C to −40°C in the updraft), and ice phase region (<−40°C).	Interpolated as necessary, using linear interpolation between reported levels. Means computed using depth-weighted means of reported values.
$\mathbf{V}_{\text{super}}$; predicted supercell motion. This quantity was found to be a poor predictor of storm motion; actual storm motions were used instead.	15 degrees to right; 85% of mean wind vector if mean windspeed > 15 m s^{-1}. 25 degrees to right; 75% otherwise (e.g., Johns et al. 1993).
SREH; storm-relative environmental helicity.	Davies-Jones (1984). Computed relative to observed storm motion as well as $\mathbf{V}_{\text{super}}$.
L; hodograph length from 0–4 km AGL.	Rasmussen and Wilhelmson (1983).
Shear vector magnitudes; BL to 1, 2, . . . , 9, 10 km.	Standard.
Storm-relative wind speed $\lvert\mathbf{V}_{\text{SR}}\rvert$; BL, 1, 2, . . . , 9, 10 km. Subscript e for environment; s for observed storm motion.	$\lvert\mathbf{V}_{\text{SR}}\rvert = [(u_e - u_s)^2 + (v_e - v_s)^2]^{0.5}$
BRN shear (Weisman and Klemp 1982).	Magnitude of shear vector from the boundary layer velocity to the 0–6-km mean wind vector.
Minimum mid level SR wind speed $\lvert\mathbf{V}_{\text{SR}}\rvert_{\text{min}}$ (Brooks et al. 1994b).	Minimum reported $\lvert\mathbf{V}_{\text{SR}}\rvert$ between 2 and 9 km AGL.
BRN; the bulk Richardson number (Weisman and Klemp 1982). Computed using (for "U"; BRN shear) shear vector magnitude from the boundary layer to 9 km AGL, and 9 km SR wind speed (in a sense an "anvil outflow" BRN).	$\text{BRN} = \frac{\text{CAPE}}{\frac{1}{2}U^2}$

itable water than their counterparts implies that these environments are also warmer in the mean.

Bluestein and Parks (1983) report significantly different mean relative humidity between their storm classes, a result that is not repeated in the present study. Many characterizations of water vapor content in soundings are strongly dependent on the depth of the surface-based "moist layer" and the absolute humidity in that layer. It is felt that the sounding climatology reported herein does not adequately sample the character of this moist layer, which is known to vary greatly on the mesoscale (Ziegler and Hane 1993). The mixing ratio of the source parcel used in CAPE calculations was based on reported surface mixing ratios, and this value should be much less sensitive to mesoscale "upwelling" of the moist layer. As shown in Fig. 5, the mixing ratio is only

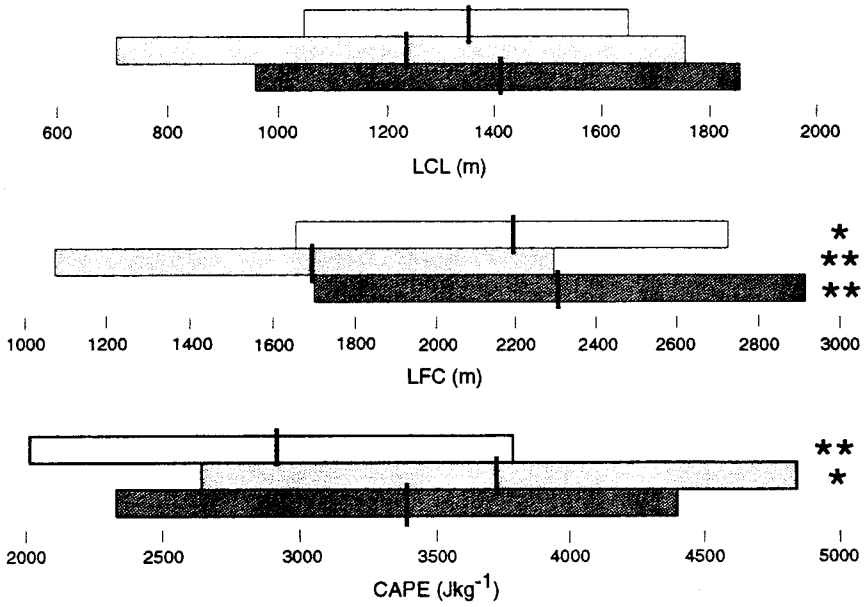

FIG. 4. Bar graphs of the distributions of LCL height (m AGL), LFC height (m AGL), and CAPE (J kg^{-1}). The black vertical ticks at the center of each bar are at the mean value, and the bar extends ± 1 standard deviation from the mean. A single asterisk beside the bar indicates that the mean is significantly different than all supercells at the 95% confidence level, and a double-asterisk indicates significance at the 98% confidence level. The white bar is for LP storms, gray for CL, and dark gray for HP.

slightly larger (not significant) in HP cases than in LP and CL cases.

Examination of the ''evaporative potential'' (see Table 2) of the storm environment yields a surprising result. In a variety of measures, HP storm environments featured the driest midlevel air, and the largest evaporative potential. For example, the ''100% extinction height'' (the height at which a fixed quantity of water proportional to the inflow mixing ratio evaporates entirely after descending from 9 km while bringing the environment to saturation at each level; Fig. 5) is significantly higher in the HP environment, and significantly closer to the surface in the CL environment. The intuitive notion of large evaporation in the LP environment and small evaporation in the HP environment is not supported in this sample. This is a difficult result to interpret, and will be discussed further in section 4.

c. Wind structure

A great variety of measures were examined that characterize the wind and shear structure of the storm environments. These were different from those utilized by BP. However, the results presented by BP indicate that shear through the depth of the troposphere is larger in LP cases than in the CL/HP class, and that low-level turning and vector shear are also larger in the former. In subsequent sections, it will be shown that low-level shear is larger in classic cases than in LP. However, the results presented herein show that it is the distribution of shear with height, and the level at which large shear occurs, that is important in determining storm type. These details can be masked when tropospheric means are computed, as was done in BP.

The physically important differences between the wind structures of the environments of the three categories of supercells is best illustrated using composite hodographs. Several compositing techniques were explored, utilizing the assumption that the important physics are related to the shear structure, not the orientation of the hodograph or displacement of the hodograph curve from the origin (i.e., the assumption that storm structure is not dependent on rotation or Galilean transformations of the hodograph). The transformation of the hodograph that seemed to be the most useful for facilitating intercomparisons was a translation so that the boundary layer mean wind (0–500 m AGL vector average) was the origin, and the boundary layer to 4 km shear vector[2] was aligned with the positive x axis. As with any compositing technique, the averaging may

[2] The choice of depth (4 km) can be made arbitrarily. The shape of the composite hodograph is the same regardless of the depth of the shear vector used to rotate it. In this case, the choice of 4 km highlighted nicely the differences among the composites. Furthermore, the average storm motion, as a vector offset from the shear vector, contains the smallest average error when based on the BL–4-km shear. This fact is being utilized in a separate study of supercell propagation.

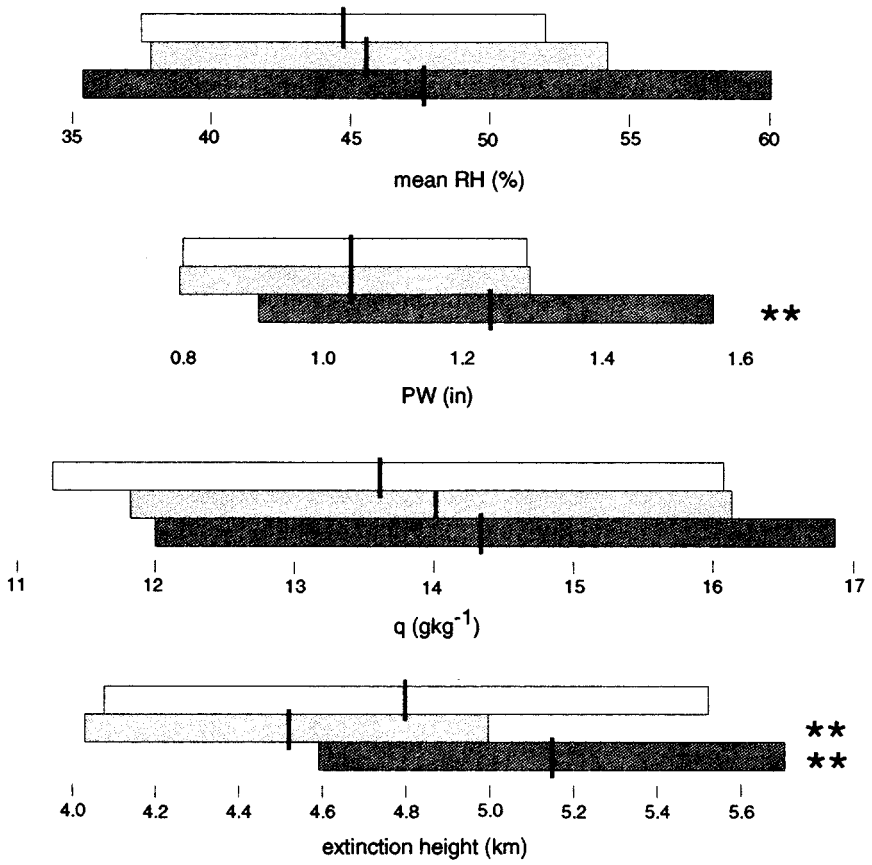

FIG. 5. Bar graphs of mean relative humidity (%; 0–5 km AGL), precipitable water (in), source parcel mixing ratio (g kg^{-1}), and extinction height (m). Symbols as in Fig. 4

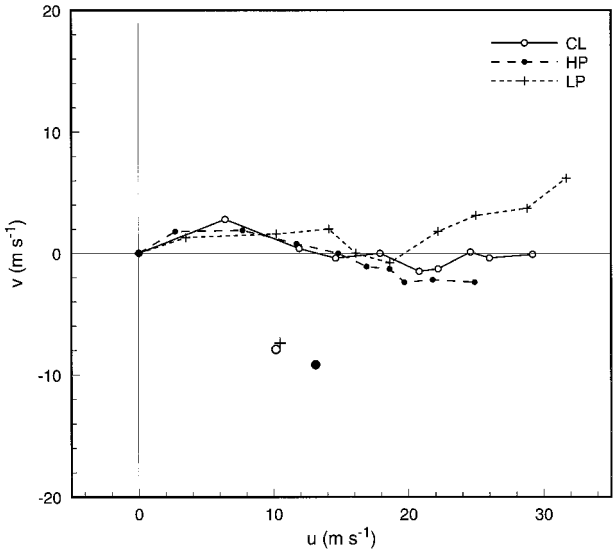

FIG. 6. Composite hodographs for the CL, HP, and LP cases. All hodographs rotated so the boundary layer to 4-km shear vector is oriented toward the east and the boundary layer mean wind is at the origin, prior to compositing. Single open circles represent the average motion of CL storms, filled circles HP storms, and plus signs LP storms.

eliminate common features that are present at different heights in the individual hodographs.

The mean hodograph for each category of storms is shown in Fig. 6. It is apparent that the most significant difference in the hodographs is in the upper troposphere, especially above about 7 km AGL. The wind in LP environments backs relatively strongly with height in upper levels, while the wind in HP environments veers slightly. The CL hodograph is in between. Considering the fact that most supercells move to the right of the lower-tropospheric shear vector, it is obvious that SR upper-tropospheric flow is strongest in the LP environment, and weakest in the HP environment. Further, precipitation descending from the forward anvil should fall farther to the left of the storm path in the case of LP storms than HP storms. This has important implications for the recirculation of precipitation particles descending from the forward-flank anvil.

As revealed in the composite hodographs, the structure of the deep-tropospheric shear magnitude is different among the three categories of supercells (Fig. 7). For example, the mean BL–9-km shear magnitude for LP storms is around 33 m s^{-1}, while for HP storms it is only about 26 m s^{-1} (significant at the 95% level as shown by the asterisks in the figure). Much of this dif-

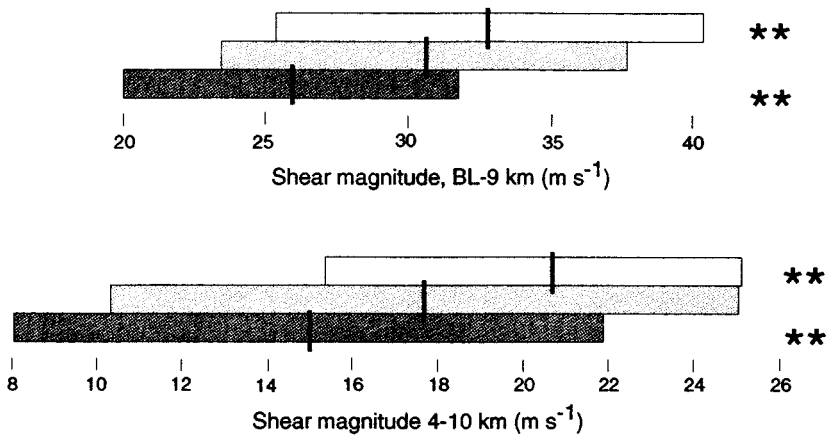

FIG. 7. Bar graphs showing the distribution of shear in the boundary layer (BL) to 9-km layer, and in the 4–10-km layer. Symbols as in Fig. 4.

ference accrues in the region above 4 km; the mean 4–10-km shear magnitudes are 22 and 15 m s^{-1}, respectively. These differences in shear are a result of both stronger winds, and the curvature to the left, in the upper-tropospheric portion of the hodographs for LP storms.

The nature of the turning of the wind vector in the upper troposphere is a fairly strong discriminator between LP and HP environments. Again utilizing the rotated, translated hodographs, the shear magnitude of the v component of the wind between 5 and 9 km is greater than zero for all LP cases, signifying a left turn to the hodograph (backing winds with height) above 5 km (Fig. 8). For HP soundings, 9 cases out of 13 have turns to the right (veering winds) in the upper troposphere. If this finding is robust, one could conclude that if the hodograph turns to the right between 5 and 9 km, LP storms will not occur, and if the hodograph turns to the left, HP storms are unlikely. The HP supercells are associated with both right and left curves, but more often with right curves (veering with height). As mentioned previously, the significance of this finding is that the backing upper winds cause the anvil to stream away to the left of the updraft's path, reducing the potential for the updraft to reingest hydrometeors. This effect is amplified by the tendency of the storm to move to the right of the BL–4-km shear vector (i.e., the storm motion contributes to the magnitude of the SR upper-tropospheric flow).

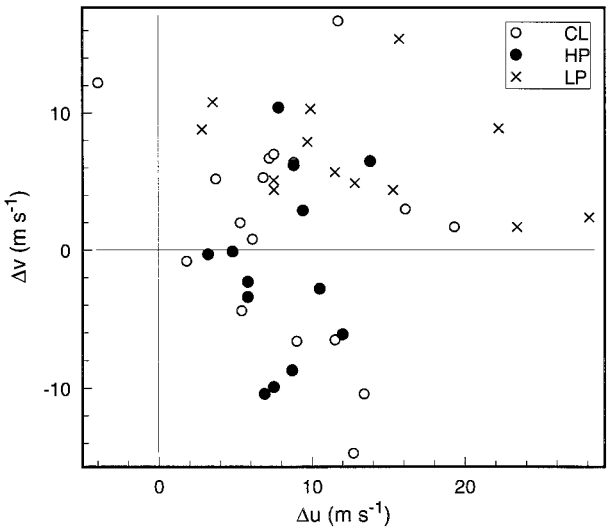

FIG. 8. Scatter diagram showing the components of shear between 5 and 9 km, in rotated and translated hodographs (see text).

This climatological analysis reveals one additional very significant finding. The rather small signals in the orientation and magnitude of the deep upper shear are enhanced by storm motion. This goes beyond the simple effect mentioned above, wherein deviant motion to the right accentuates the effect of the upper-tropospheric left turn. In fact, the LP storms in this study propagated more slowly and further to the right than the other storms, further enhancing the SR upper flow. While HP storms propagated much more erratically, several of these storms tended to propagate more rapidly and in a direction more along the BL–4-km shear vector, so that the SR upper-tropospheric flow was reduced further. Thus, the type of supercell that occurs may be strongly influenced by the motion of the storm itself. These differences in propagation are the subject of an ongoing investigation.

When the flow is examined in the SR framework, these differences between the classes of storms become obvious. The SR flow for all cases is summarized in Fig. 9. It is apparent that the upper-tropospheric SR flow is strongest in the LP cases with the SR flow increasing strongly from 4 to 10 km above ground level (AGL). In sharp contrast, the HP cases reveal a nearly constant SR wind speed from the boundary layer to the upper troposphere. The CL cases fall between these two extremes, with peak upper-tropospheric winds about the same as in the LP cases, but the increase in SR flow

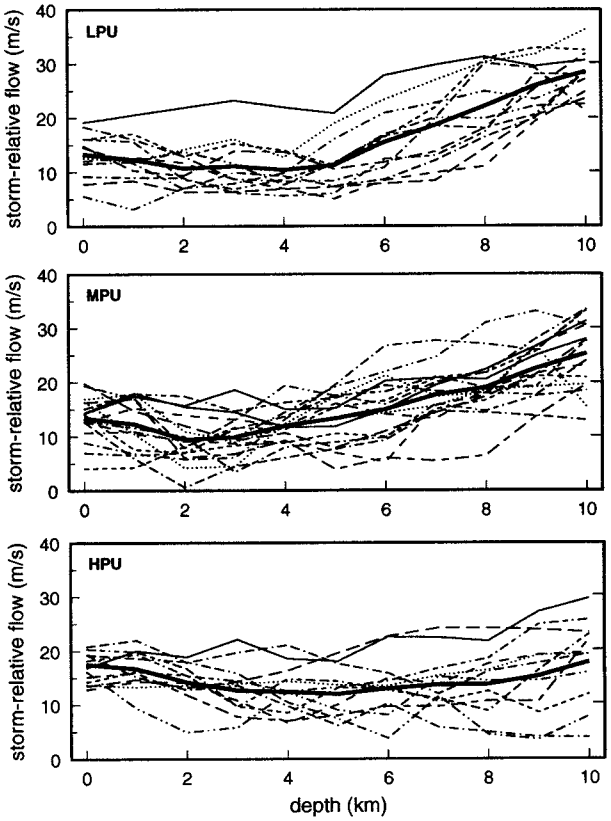

FIG. 9. Storm-relative (SR) wind speed (m s^{-1}) for all cases. The top graph is for LP storms, the middle for CL storms, and the bottom for HP storms. Heavy curves represent the mean for each storm type.

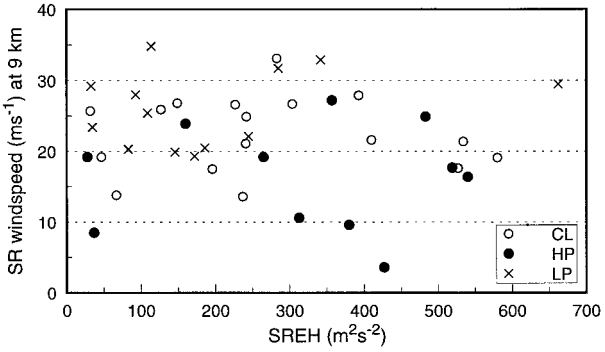

FIG. 10. Scatter diagram of storm-relative environmental helicity (SRH) versus storm-relative wind speed at 9 km.

occurs more gradually and is spread between 2 and 10 km AGL.

Note that the SR flow from 2 to 7 km AGL differs among the classes by only 1–3 m s^{-1}, and that the significant differences emerge between about 8 and 10 km. Among all classes, most storms have relatively weak ($\sim$10 m s^{-1}) SR flow near 4–6 km AGL. This finding would tend to contradict the finding in Brooks et al. (1994b) that differences in the location of precipitation are strongly dependent on the middle-tropospheric SR flow; the evidence presented herein clearly shows that the strong dependence is on upper-tropospheric flow. Brooks et al. (1994a) couple the middle-tropospheric SR wind speed, SRH, and maximum sounding mixing ratio to evaluate the difference between the environments of tornadic versus nontornadic supercells, utilizing the assumption that the distribution of precipitation plays a strong role in allowing or preventing tornadogenesis. The same parameter space was examined in the present study, since the emphasis here also is on precipitation distribution. However, no significant differences could be found among the classes of supercells. This will be discussed further in section 4.

The 9–10-km level is the level at which numerical simulations typically indicate the updraft nondivergence level resides, and several recently obtained airborne Doppler datasets indicate that this is the level at which the supercell anvil begins spreading away from the updraft. Hence, it seems that the finding of the importance of the 9–10-km SR flow supports the hypothesis that the anvil-layer transport of hydrometeors away from the updraft plays a vital role in determining the degree to which hydrometeors are reingested into the updraft leading to augmented precipitation in that region. [Climatologically the tropopause during spring is around 11 km AGL. Because the wind vector can change rapidly at and above the tropopause, it is not surprising that, in this study, the strongest signal associated with upper-tropospheric flow is around 9–10 km AGL (note that supercells almost always reach to heights above the tropopause).]

It appears that SRH does have a significant association with storm type. This is illustrated in Fig. 10. With SR upper flow of less than about 12 m s^{-1}, supercells are exclusively of the HP variety (when supercells even exist) regardless of SRH. Similarly, with SR upper flow of $>$30 m s^{-1}, most supercells are LP. In between, especially in the range of SR upper flow between about 18 and 28 m s^{-1}, supercells in environments with small SRH ($\lesssim$250 m^2 s^{-2}) tend to be LP, and as SRH increases, the storms tend toward the HP part of the spectrum. As already discussed, HP supercells tend to move more rapidly than their LP counterparts, which largely accounts for the greater magnitude of SRH with these storms. The finding of the association of SRH with supercell type is discussed further in light of a similar numerical finding by Brooks et al. (1994b) in section 4.

Finally, a small difference in lower-tropospheric wind structure among the three classes is evident from the data already presented (Fig. 6). The lower-tropospheric shear is weakest in the HP cases. The shear is stronger in the LP cases, but the hodograph is relatively straight. The most curved composite hodograph, with the largest shear magnitude, is associated with CL storms. This finding is presented for completeness; it is felt that mesoscale variations in low-level flow in the supercell en-

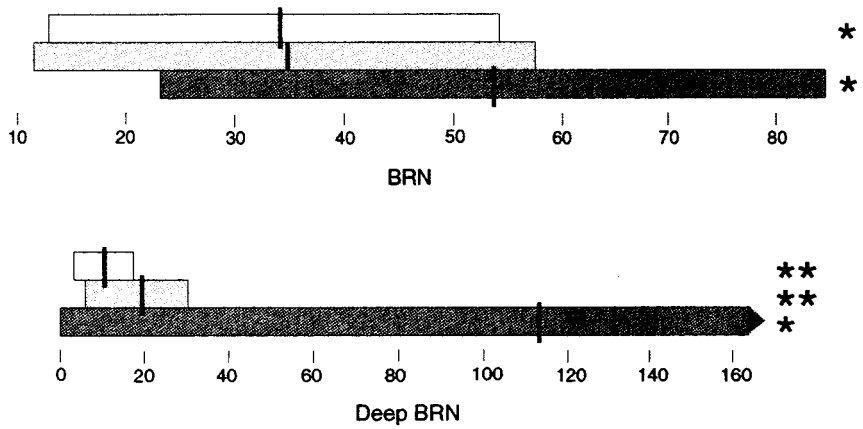

FIG. 11. Bar graphs showing the distribution of (a) bulk Richardson number, and (b) deep bulk Richardson number. Symbols as in Fig. 4.

vironment may be so large (e.g., Davies-Jones 1993) that the findings based on this sounding climatology may be dubious.

d. Combinations of shear and thermodynamic parameters

Several studies have argued that the bulk Richardson number (BRN; Weisman and Klemp 1982) lacks utility in forecasting supercells and tornadoes (Johns et al. 1993). However, in a simple sense, a form of the BRN *should* be useful for predicting supercell type. This is because the BRN is smaller when CAPE is relatively small and shear is large, a condition that may favor transport of hydrometeors far from the updraft and hence LP supercells (given sufficient CAPE). Conversely, very weak shear or large CAPE would emphasize the vertical branch of hydrometeor transport, and favor HP storms. As formulated by Weisman and Klemp (1982), however, the BRN is dependent on the flow structure in the lowest 6 km only, and hence misses the important flow magnitude in the upper troposphere. In Fig. 11, the Weisman and Klemp form of the BRN is compared to a form based on the results herein. The form of BRN in Eq. (1) will be called the deep bulk Richardson number (DBRN), where U_9 is the magnitude of the shear vector between the boundary layer and 9 km AGL. It is apparent from Fig. 9 that this form *is* of potential value in discriminating between supercell environments:

$$\text{DBRN} = \frac{\text{CAPE}}{\frac{1}{2}U_9^2}. \tag{1}$$

4. Discussion

The data presented above indicate that the SR flow is different from one part of the supercell spectrum to another. In particular, SR environmental flow at the anvil level is much stronger for LP storms than HP, with the environments supporting CL storms having intermediate upper-flow strengths. Further, the SR wind speed differential between about 4 km and 9 km is much larger in LP environments than HP. The composite hodographs of LP storms favor the deposition of hydrometeors much farther to the left of the storm track than those for HP storms.

The CAPE of the supercell environment (~3000 J kg^{-1}) supports updrafts of several tens of meters per second. It is commonly believed that about 10–30 min are required for precipitation formation in a supersaturated parcel (e.g., Young 1993), but the residence time of a parcel in a supercell updraft core probably is around 10 min or less. Thus, precipitation in the proximity of supercell updrafts probably is due to the ingestion of hydrometeors from outside the updraft, which subsequently collect large amounts of supercooled water and grow to sizes sufficient to descend through the updraft, as well as to precipitation growth in the fringes of the updraft where parcel residence time is greater (Yuter and Houze 1995). It appears that the strong SR upper flow of the LP environment tends to transport hydrometeors well away from the updraft, greatly reducing the number that are reingested in the updraft, and hence greatly limiting the production of precipitation in the updraft itself. Further, this paucity of precipitating hydrometeor embryos greatly reduces the competition for liquid water in the updraft, which explains the frequent observation that hail (often very large stones) is the only or dominant precipitation type near the updraft of LP storms. The much weaker SR upper flow near HP storms allows many more hydrometeors to be ingested into the updraft, leading to much greater precipitation rates in much of the updraft region. With very weak SR upper flow, hydrometeors may never be removed from the updraft at all. The precipitation physics described above are the subject of a modeling study, with the results of that study to be reported in Part II of this paper.

Based on the findings in section 3, a number of observations concerning the supercell spectrum can be explained. First, LP storms have been associated with the dryline environment (e.g., Burgess and Davies-Jones 1979; BP), whereas CL storms have been associated with the Great Plains ''transitional environment'' (Moller et al. 1994), and HP storms tend to be the dominant supercell type across the entire United States (Doswell et al. 1990). This geographical distribution possibly is due to the coverage of the convection itself. If the hypothesis is correct, and supercell precipitation characteristics are a strong function of the amount of hydrometeors reingested into the updraft, then storms would tend toward the HP end of the spectrum whenever they are overtaken by other cells, the anvils from other cells, or perhaps even thick cirrus [this may explain the sharp LP/HP demarcation in the case discussed by Branick and Doswell (1992, 148)]. This mechanism would operate regardless of the strength of the SR upper flow (recall that the cases chosen for this paper were isolated storms in order to isolate the effects of environmental flow from the effects of the presence of other storms). The upstream (with respect to upper flow) limit of the occurrence of convection tends to be the dryline or an eastward-progressing cold front. Convective cells and anvils generally are not present upstream of these boundaries, so the storm type near these boundaries is largely determined by the SR upper flow. Thus it is to be expected that LP storms would be much more likely near this western extent of convective development. Farther east, it becomes increasingly likely that there are storms upstream of any given supercell, which will provide hydrometeors for ingestion into the updraft and force the storms toward the HP end of the spectrum. Therefore it seems reasonable that HP storms should dominate in all regions away from the dryline; this possibility merits further investigation.

Similarly, it is possible that convection is much more widespread in the eastern United States compared to the Great Plains because of the nature of the ''lid'' (R. Davies-Jones 1997, personal communication). For example, if the lid is climatologically stronger in the central United States, storms might be more isolated in general compared to regions where the lid is weaker. More widespread convection in regions with weaker lids would favor HP storms through seeding between storms.

It has been observed by the authors that the same environment can support storms of markedly different types. This can also be seen in various case studies in the literature (e.g., Davies-Jones et al. 1976). Typically, the most-upstream storm will be toward the LP part of the spectrum, while all storms farther downstream tend toward the HP end. Storm type can have a strong influence on the type and likelihood of severe weather (Moller et al. 1994), so this finding should aid in the storm diagnosis and warning process.

It should be noted that a supercell should generally move *toward* the HP end of the spectrum as it evolves, even with a steady upper flow. A timescale on the order of 20 min is involved in the first development of hydrometeors aloft, their subsequent transport downwind in the anvil layer, their descent, and possible reingestion into the updraft. Thus, most supercells, at least for a short while, should be LP-type storms. If the subanvil air is particularly dry, it may take an additional period of time to become moist enough to allow hydrometeors to descend to a level at which they can be reingested without being evaporated first. Once the humidity of the subanvil layer becomes high enough, the storm may progress toward the HP end of the spectrum. In a similar process, if the large-scale environment becomes more humid or the low-level moist layer becomes deeper as the storm propagates, it should tend toward the HP end of the spectrum [such behavior has been documented by Burgess and Curran (1985)]. This is particularly true near the dryline, which by definition is the western edge of the low-level moisture and the low-level moist layer can be quite shallow just ahead of the dryline, while deepening farther east (Schaefer 1973). Further, some supercells are not isolated convective cells at their inception [e.g., the multicell to supercell evolution described by Vasiloff (1986)], and the prior existence of other convective cells could play an important role in determining the precipitation character of the mature supercell.

Somewhat differing from the findings of Brooks et al. (1994a,b), the data presented herein indicate that the midlevel SR flow is generally 10–15 m s^{-1} in all supercell types, while it is the anvil-level SR flow that is most important in terms of precipitation distribution near the updraft. This finding will be explored with a new cloud model in Part II of this set of papers. It appears that the difference in findings can be attributed to certain limitations inherent in the numerical model and sounding used in Brooks et al. (1994b). For example, they did not vary the flow above 7 km AGL, so any sensitivities to upper-tropospheric flow strength were not explored. However, gravitational sorting in the presence of shear will cause slow-falling hydrometeors to be deposited relatively farther away from the updraft, implying that it is the SR flow in the layers containing slow-falling hydrometeors (e.g., above 7 km) that is most important. Kessler-type microphysics only allow for relatively fast-falling rain, biasing the precipitation distribution toward the updraft, again owing to gravitational sorting in shear. Finally, Kessler microphysics parameterizations allow precipitation formation in air parcels much sooner than what is observed in nature (immediately upon supersaturation in the Kessler scheme, while in real clouds the diffusional and coalescence growth processes enforce a timescale of >10 min for precipitation formation in supersaturated parcels). This also biases the precipitation distribution toward the updraft where precipitation forms too early and low. The combination of these three effects would lead to much precipitation formation in and near the

lower one-half of the updraft, so the important SR flow for hydrometeor redistribution in the cloud model would be in middle levels instead of the upper troposphere.

With regard to the role of SRH and the inferred mesocyclone intensity, the findings herein indicate that large SRH (computed for each case, and implied by the composite low-level hodograph shapes and shear intensity) may be associated with a tendency toward the HP end of the spectrum. This issue will require a great deal of additional investigation: for example, does the more rapid motion of HP storms lead to larger SRH, or does the SRH lead to an HP storm that intrinsically moves more quickly? It is plausible [as argued by Brooks et al. (1994b)] that the mesocyclones tend to reduce midlevel SR flow and enhance low-level inflow. According to the hypothesis discussed here, this would increase the likelihood of anvil hydrometeors being reingested into the updraft (especially on the left side), increasing precipitation production there. Regardless of the precipitation physics involved (redistribution of updraft-generated ''primary'' precipitation, or increasing the likelihood of ingestion of ''secondary'' hydrometeors), the net effect of mesocyclone strength appears to be to move storms toward the HP end of the spectrum.

Inherent in the hypothesis being evaluated, supercell type depends on the degree to which hydrometeors descending from the anvil are reingested into the updraft. Intuitively, this should depend further on the subanvil evaporation potential. The sounding data did not provide a clear signal that this is the case. However, it is important to understand that subanvil evaporation will be influenced by many factors not measured here; among these are the real depth of the moist layer, the SR subanvil flow immediately downstream of the updraft and thus the potential to advect moistened air away from the storm, and other factors. From an observational perspective, further field research on the horizontal distribution of water vapor in the subanvil layer, and in situ microphysical measurements apparently will be required to evaluate the importance of subanvil evaporation.

It is obviously an oversimplification to assume that the only source for precipitation embryos in a supercell updraft is the downshear anvil. These hydrometeors could easily be produced in the upshear anvil or in other parts of the near-updraft region (e.g., Foote 1984; Knight and Knupp 1986; Miller et al. 1988; Yuter and Houze 1995). However, the findings of this analysis do tend to support the idea that strong anvil-level SR flow transports the bulk of primary hydrometeors away from the updraft, wherever they originally form.

It is hoped that these findings can be further evaluated for a much expanded set of storms. Any such effort would benefit greatly through the use of an objective technique (preferably radar based) to assess the storm type, in terms of both precipitation intensity in the updraft/mesocyclone region, and in the forward-flank anvil region. An expanded climatology should attempt to include cases with even stronger SR anvil-level flow than the range investigated here, and should perhaps focus on the character of flanking lines in isolated supercells. This is because observations by the authors during VORTEX-95 (Rasmussen et al. 1994) indicate that in very strong shear, supercells tended to be accompanied by very long flanking lines of cells that may have ''seeded'' the primary updrafts and forced the storms toward the HP end of the spectrum.

Acknowledgments. We wish to acknowledge Greg Stumpf (NSSL) and David Blanchard (CIMMS/NSSL) for their contributions of information about various supercells they have observed. This work benefited greatly from careful reviews by two anonymous reviewers as well as by Drs. Bob Davies-Jones and Bob Maddox of NSSL. Discussions with Drs. Brooks and Doswell of NSSL also were helpful. Photographs were contributed by Warren Faidley (Weatherstock) and Phillip Spencer (NSSL). This work was supported in part by National Science Foundation Grants ATM-9311911, ATM-9120009, and ATM-9617318, and by the Cooperative Institute for Mesoscale Meteorology.

REFERENCES

Bluestein, H. B., 1984: Further examples of low-precipitation severe thunderstorms. *Mon. Wea. Rev.,* **112,** 1885–1888.

——, and C. R. Parks, 1983: A synoptic and photographic climatology of low-precipitation severe thunderstorms in the Southern Plains. *Mon. Wea. Rev.,* **111,** 2034–2046.

——, and G. R. Woodall, 1990: Doppler-radar analysis of a low-precipitation severe storm. *Mon. Wea. Rev.,* **118,** 1640–1664.

Branick, M. L., and C. A. Doswell III, 1992: An observation of the relationship between supercell structure and lightning ground-strike polarity. *Wea. Forecasting,* **7,** 143–149.

Brooks, H. B., and R. B. Wilhelmson, 1992: Numerical simulation of a low-precipitation supercell thunderstorm. *Meteor. Atmos. Phys.,* **49,** 3–17.

——, C. A. Doswell III, and J. Cooper, 1994a: On the environments of tornadic and nontornadic mesocyclones. *Wea. Forecasting,* **9,** 606–618.

——, ——, and R. B. Wilhelmson, 1994b: The role of midtropospheric winds in the evolution and maintenance of low-level mesocyclones. *Mon. Wea. Rev.,* **122,** 126–136.

Browning, K. A., 1964: Airflow and precipitation trajectories within severe local storms which travel to the right of the winds. *J. Atmos. Sci.,* **21,** 634–639.

——, 1977: The structure and mechanism of hailstorms. *Hail: A Review of Hail Science and Hail Suppression, Meteor. Monogr.,* No. 38, Amer. Meteor. Soc., 1–43.

——, and R. J. Donaldson, 1963: Airflow and structure of a tornadic storm. *J. Atmos. Sci.,* **20,** 533–545.

——, and G. B. Foote, 1976: Airflow and hail growth in supercell storms, and some implications for hail suppression. *Quart. J. Roy. Meteor. Soc.,* **102,** 499–533.

Burgess, D. B., and R. P. Davies-Jones, 1979: Unusual tornadic storms in eastern Oklahoma on 5 December 1975. *Mon. Wea. Rev.,* **107,** 451–457.

——, and E. B. Curran, 1985: The relationship of storm type to environment in Oklahoma on 26 April 1984. Preprints, *14th Conf. on Severe Local Storms,* Indianapolis, IN, Amer. Meteor. Soc., 208–211.

Davies-Jones, R. P., 1984: Streamwise vorticity: The origin of updraft rotation in supercell storms. *J. Atmos. Sci.,* **41,** 2991–3006.

——, 1993: Helicity trends in tornado outbreaks. Preprints, *17th Conf. on Severe Local Storms,* St. Louis, MO, Amer. Meteor. Soc., 56–60.

——, and H. E. Brooks, 1993: Mesocyclogenesis from a theoretical perspective. *The Tornado: Its Structure, Dynamics, Prediction, and Hazards, Geophys. Monogr.,* Amer. Geophys. Union, 105–114.

——, D. W. Burgess, and L. R. Lemon, 1976: An atypical tornado-producing cumulonimbus. *Weather,* **31,** 336–347.

Donaldson, R., A. Spatola, and K. Browning, 1965: Visual observations of severe weather phenomena. A family outbreak of severe local storms—A comprehensive study of the storms in Oklahoma on 26 May 1963. Part I. Air Force Cambridge Research Lab., Spec. Rep. No. 32, 73–97. [Available from AFGL, Hanscomb AFB, MA 01731.]

Doswell, C. A., and D. W. Burgess, 1993: Tornadoes and tornadic storms: A review of conceptual models. *The Tornado: Its Structure, Dynamics, Prediction, and Hazards, Geophys. Monogr.,* Amer. Geophys. Union, 161–172.

——, A. R. Moller, and R. Przybylinski, 1990: A unified set of conceptual models for variations on the supercell theme. Preprints, *16th Conf. Severe Local Storms,* Kananaskis Park, AB, Canada, Amer. Meteor. Soc., 40–45.

Foote, G. B., 1984: Study of hail growth utilizing observed storm conditions. *J. Climate Appl. Meteor.,* **23,** 84–101.

Forbes, G. S., 1981: On the reliability of hook echoes as tornado indicators. *Mon. Wea. Rev.,* **109**, 1457–1466.

Johns, R. H., J. M. Davies, and P. W. Leftwich, 1993: Some wind and instability parameters associated with strong and violent tornadoes. Part II: Variations in the combinations of wind and instability parameters. *The Tornado: Its Structure, Dynamics, Prediction, and Hazards, Geophys. Monogr.,* Amer. Geophys. Union, 583–590.

Klemp, J. B., 1987: Dynamics of tornadic thunderstorms. *Annu. Rev. Fluid Mech.,* **19,** 369–402.

——, and R. Rotunno, 1983: A study of the tornadic region within a supercell thunderstorm. *J. Atmos. Sci.,* **40,** 359–377.

——, R. B. Wilhelmson, and P. S. Ray, 1981: Observed and numerically simulated structure of a mature supercell thunderstorm. *J. Atmos. Sci.,* **38,** 1558–1580.

Knight, C. A., and K. R. Knupp, 1986: Precipitation growth trajectories in a CCOPE storm. *J. Atmos. Sci.,* **43,** 1057–1073.

Lemon, L. R., 1982: New severe thunderstorm radar identification techniques and warning criteria: A preliminary report. NOAA Tech. Memo. NWS NSSFC-1, 60 pp. [NTIS PB-273049.]

——, and C. A. Doswell III, 1979: Severe thunderstorm evolution and mesocyclone structure as related to tornadogenesis. *Mon. Wea. Rev.,* **107,** 1184–1197.

Maddox, R. A., 1976: An evaluation of tornado proximity wind and stability data. *Mon. Wea. Rev.,* **104,** 133–142.

Marwitz, J. D., 1972: The structure and motion of severe hailstorms. Part III: Severely sheared storms. *J. Appl. Meteor.,* **11,** 189–201.

Miller, L. J., J. D. Tuttle, and C. A. Knight, 1988: Airflow and hail growth in a severe northern High Plains supercell. *J. Atmos. Sci.,* **45,** 736–762.

——, ——, and G. B. Foote, 1990: Precipitation production in a large Montana hailstorm: Airflow and particle growth trajectories. *J. Atmos. Sci.,* **47,** 1619–1646.

Moller, A. R., C. A. Doswell III, and R. Przybylinski, 1990: High-precipitation supercells: A conceptual model and documentation. Preprints, *16th Conf. on Severe Local Storms,* Kananaskis Park, AB, Canada, Amer. Meteor. Soc., 52–57.

——, ——, M. P. Foster, and G. R. Woodall, 1994: The operational recognition of supercell thunderstorm environments and storm structures. *Wea. Forecasting,* **9,** 327–347.

Paluch, I. R., 1978: Size sorting of hail in a three-dimensional updraft and implications for hail suppression. *J. Appl. Meteor.,* **17,** 763–777.

Proctor, F. H., 1983: Numerical simulation of a bell-shaped cumulonimbus. Preprints, *13th Conf. on Severe Local Storms,* Tulsa, OK, Amer. Meteor. Soc., 235–240.

Rasmussen, E. N., J. M. Straka, R. Davies-Jones, C. A. Doswell III, F. H. Carr, M. D. Eilts, and D.R. MacGorman, 1994: Verifications of the Origins of Rotation in Tornadoes Experiment: VORTEX. *Bull. Amer. Meteor. Soc.,* **75,** 995–1006.

Rotunno, R., and J. B. Klemp, 1982: The influence of the shear-induced pressure gradient on thunderstorm motion. *Mon. Wea. Rev.,* **110,** 136–151.

——, and ——, 1985: On the rotation and propagation of numerically simulated supercell thunderstorms. *J. Atmos. Sci.,* **42,** 271–292.

Schaefer, J. T., 1973: The motion and morphology of the dryline. NOAA Tech. Memo ERL NSSL-66, 81 pp. [NTIS COM-74-10043.]

Vasiloff, S. V., 1986: Investigation of the transition from multicell to supercell storms. *J. Climate Appl. Meteor.,* **25,** 1022–1036.

Weisman, M. L., and J. B. Klemp, 1982: The dependence of numerically simulated convective storms on vertical wind shear and buoyancy. *Mon. Wea. Rev.,* **110,** 504–520.

——, and ——, 1984: The structure and classification of numerically simulated convective storms in directionally varying wind shears. *Mon. Wea. Rev.,* **112,** 2479–2498.

——, and H. B. Bluestein, 1985: Dynamics of numerically simulated LP storms. Preprints, *15th Conf. on Severe Local Storms,* Indianapolis, IN, Amer. Meteor. Soc., 167–171.

——, and ——, 1986: Characteristics of isolated convective storms. *Mesoscale Meteorology and Forecasting,* P. Ray, Ed., Amer. Meteor. Soc., 331–358.

Wilhelmson, R. B., and J. B. Klemp, 1978: A three-dimensional numerical simulation of splitting that leads to long-lived storms. *J. Atmos. Sci.,* **35,** 1037–1063.

Young, K. C., 1993: Microphysical Processes in Clouds. Oxford University Press, 427 pp.

Yuter, S. E., and R. A. Houze Jr., 1995: Three-dimensional kinematic and microphysical evolution of Florida cumulonimbus. Part I: Spatial distribution of updrafts, downdrafts, and precipitation. *Mon. Wea. Rev.,* **123,** 1921–1940.

Ziegler, C. L., and C. E. Hane, 1993: An observational study of the dryline. *Mon. Wea. Rev.,* **121,** 1134–1151.

——, P. S. Ray, and N. C. Knight, 1983: Hail growth in an Oklahoma multicell storm. *J. Atmos. Sci.,* **40,** 1768–1791.